

DISCRETE OPTIMAL TRANSPORT IS A STRONG AUDIO ADVERSARIAL ATTACK

A. Selitskiy,¹ A. Shahriyar,² and J. Prakasan²

¹University of Rochester, ²Rochester Institute of Technology

ABSTRACT

In this paper, we show that *discrete optimal transport* (DOT) is an effective black-box adversarial attack against modern audio anti-spoofing countermeasures (CMs). Our attack operates as a post-processing, distribution-alignment step: frame-level WavLM embeddings of generated speech are aligned to an unpaired bona fide pool via entropic OT and a top- k barycentric projection, then decoded with a neural vocoder. Evaluated on ASVspoof2019 and ASVspoof5 with AASIST baselines, DOT yields consistently high equal error rate (EER) across datasets and remains competitive after CM fine-tuning, outperforming several conventional attacks in cross-dataset transfer. Ablation analysis highlights the practical impact of vocoder overlap. Results indicate that distribution-level alignment is a powerful and stable attack surface for deployed CMs.

Index Terms— Optimal transport, adversarial attack, ASVspoof

1. INTRODUCTION

Vector-embedding voice conversion (VC) with WavLM model [1] began with a simple k -nearest neighbors (k NN) mapping in embedding space [2]. Subsequent work replaced k NN with *optimal transport* (OT), improving alignment between source and bona fide target distributions and refining conversion quality [3, 4]. In particular, discrete OT (DOT) with barycentric projection was recently applied as a *post-processing domain-alignment* step on generated audio, yielding scores close to genuine recordings under strong countermeasures (CMs) [4]. OT has likewise been explored on the *defense* side for distribution comparison in anti-spoofing [5].

A large body of work has shown that automatic speech recognition (ASR) and speaker verification (ASV) pipelines are vulnerable to adversarial examples, including optimization-based attacks like [6] (see also [7, Sec. 7]). In parallel, the ASVspoof challenges established standardized corpora and protocols (e.g., ASVspoof2019 [8]; ASVspoof5 [7]) for training and evaluating spoofing CMs. Among modern CMs, AASIST systems [9] and its modifications leverage spectro-temporal graph attention to capture diverse spoofing

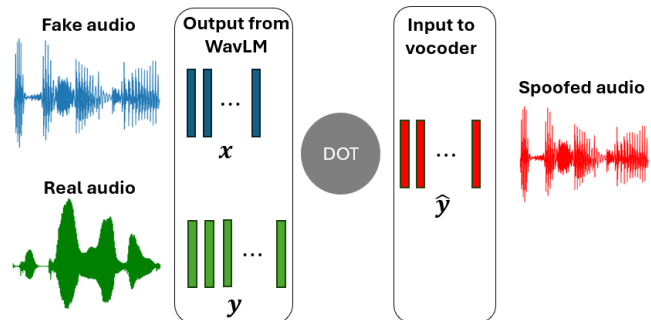


Fig. 1. Discrete OT adversarial attack system overview.

artifacts and have become strong baselines for deepfake/anti-spoofing detection. Despite this progress, transferability across datasets and generative models remains an open challenge.

We study whether *discrete OT*-based voice conversion is a strong black-box attack on state-of-the-art CMs (Figure 1). Our method aligns WavLM frame embeddings to an unpaired bona fide pool via entropic DOT with a cosine cost, applies a top- k barycentric map, and reconstructs with a neural vocoder. Unlike gradient attacks, DOT induces a *distributional shift* toward bona fide regions, enabling cross-dataset transfer without CM internals. **Our Contributions:**

- **DOT as an adversarial attack.** We formalize discrete OT + barycentric projection VC as a black-box, distribution-alignment attack.
- **Transfer and fine-tuning robustness.** DOT remains strong across datasets ASVspoof2019 and ASVspoof5 and remains competitive after CM fine-tuning, outperforming several conventional attacks.
- **Ablations and practical factors.** We show that *vocoder overlap* with CM training data modulates attack strength, informing both attack design and CM training.

2. PROBLEM SETUP AND THREAT MODEL

We consider an audio assistant/ASV pipeline with a spoofing CM trained under ASVspoof protocols [8, 7]. Given waveform x , the CM outputs a score $f(x)$; a threshold τ yields a binary (bona fide/spoof) decision.

Adversary Goal. Transform a generated/converted input x_{gen} into an attacked sample y that (i) is accepted as bona fide by the CM and (ii) preserves intelligibility/naturalness to avoid human suspicion.

Adversary Knowledge and access. We assume a black-box CM: no gradients or internals; score/label access is optional and not required. The adversary may synthesize x_{gen} using any upstream TTS/VC system, and has an *unpaired* bona fide speech pool from the target domain or a close proxy, reflecting realistic deployments and standard adversarial-audio practice.

Adversary Capabilities (DOT attack). The adversary embeds x_{gen} into frame-level vectors $X = \{x_i\}_{i=1}^M$, embeds an unpaired bona fide pool $Y = \{y_j\}_{j=1}^N$, computes an *entropic discrete OT* coupling matrix $\gamma \in \mathbf{R}^{M \times N}$ under cosine cost $c(x, y) = 1 - \cos(x, y)$, applies a *top- k barycentric projection* to obtain transported embeddings $\hat{Y} = \{\hat{y}_i\}_{i=1}^M$, and reconstructs a waveform \tilde{x} via a neural vocoder. The pipeline uses only generic pretrained components and unpaired speech.

Perceptual Constraints. The attack seeks minimal perceptual deviation from x_{gen} while achieving CM evasion.

We follow ASVspoof protocols [8, 7]. Success is demonstrated by higher EER (or higher false-acceptance rate) on \tilde{x} than baselines, including under *cross-dataset transfer* and after *CM fine-tuning*. We also analyze practical factors — *vocoder overlap*, *top- k* , and target duration — that modulate attack strength (see Sec 5).

3. METHODOLOGY: DISCRETE OT ATTACK

3.1. Discrete OT and Barycentric Projection

Let $(X, \mathcal{P}, \mathbf{P})$ and $(Y, \mathcal{Q}, \mathbf{Q})$ be two probability spaces. Denote by $\Pi(\mathbf{P}, \mathbf{Q})$ all joint distributions on the product space $(X \times Y, \mathcal{P} \otimes \mathcal{Q}, \pi)$ with marginals \mathbf{P} and \mathbf{Q} . In *discrete case* assume there are M vectors in X and N vectors in Y with probability masses $p_i = \mathbf{P}(x_i)$ and $q_j = \mathbf{Q}(y_j)$. The joint distribution $\pi(x, y)$ is represented as a non-negative matrix γ with $\gamma_{ij} = \pi(x_i, y_j)$, $i = 1, \dots, M$ and $j = 1, \dots, N$.

The goal of optimal transport (OT) is to find the joint distribution $\pi \in \Pi(\mathbf{P}, \mathbf{Q})$ known as *Kantorovich plan*, that minimizes the expected transport cost

$$\sum_i^M \sum_j^N \gamma_{ij} c(x_i, y_j) \rightarrow \inf_{\gamma_{ij}} \quad (1)$$

subject to the marginal constraints:

$$p_i = \sum_{j=1}^N \gamma_{ij} \quad \text{and} \quad q_j = \sum_{i=1}^M \gamma_{ij}. \quad (2)$$

Given a solution γ , a transport map can be defined via the

barycentric projection:

$$T(x_i) = \sum_{j=1}^N \tilde{\gamma}_{ij} y_j, \quad \text{where } \tilde{\gamma}_{ij} = \frac{\gamma_{ij}}{p_i}. \quad (3)$$

This transform can be interpreted as the conditional expectation $\mathbf{E}[y|x = x_i]$.

3.2. Adversarial Attack

We follow the discrete OT voice-conversion framework of [4]. Let one audio recording be represented by a sequence of embeddings $\mathbf{x} = [x_1, x_2, \dots, x_M]$. Here, x_i , $i = 1, \dots, M$, are embeddings obtained with WavLM Large pretrained model [1]. This model encodes every 25 ms of audio into a 1024-dimensional vector embedding, with a hop size of 20 ms.

For every pair of audio recordings (x, y) from the source and target speakers respectively, we extract their vectorized representations: \mathbf{x} and \mathbf{y} , with $x_i, y_j \in \mathbf{R}^{1024}$.

Since the underlying distributions of speaker embeddings $X = \{x_i\}_{i=1}^M$ and $Y = \{y_j\}_{j=1}^N$ are unknown, we use *empirical distributions*: $\mathbf{P}(x_i) = \frac{1}{M}$ and $\mathbf{P}(y_j) = \frac{1}{N}$. It was noticed that it is better to have a longer recording for the target speaker; therefore, Y can contain embeddings from several audio samples.

The goal is to enhance generated audio x_{gen} applying the OT form embeddings \mathbf{x} to a real sample \mathbf{y} . In other words, we want to define a mapping (transportation map) T such that $T(\mathbf{x}) \approx \mathbf{y}$, where \mathbf{y} has a similar distribution to \mathbf{Q} (but it is not necessary an element of Y). In the discrete OT approach, we compute the coupling matrix γ for the given marginal distributions and a cost function. For each x_i , we sort the target embeddings y_j in decreasing order of γ_{ij} , denoting the sorted vectors as $y_j^{\text{ot}(i)}$. The sorted coupling weights along each row (with fixed i) are denoted by $\gamma_{ij}^{\text{sort}}$.

We define the mapping \hat{T} as the barycentric projection of the OT map over top- k vectors,

$$x_i \mapsto \hat{y}_i = \sum_{j=1}^k \tilde{\gamma}_{ij}^{\text{sort}} y_j^{\text{ot}(i)}, \quad \tilde{\gamma}_{ij}^{\text{sort}} = \frac{\gamma_{ij}^{\text{sort}}}{\sum_{s=1}^k \gamma_{is}^{\text{sort}}}. \quad (4)$$

Note that this formula coincides with (3) only when $k = N$. We use $k = 5$, as it was shown in [4], the quality of conversion does not change much for $3 \leq k \leq 10$, but it degrades for large k . After the transformation $\mathbf{x} \mapsto \hat{\mathbf{y}}$, we convert the predicted embeddings $\hat{\mathbf{y}}$ back into waveform \hat{y} using HiFi-GAN vocoder (see Sec. 4).

The intuition behind this attack is simple: the approximate map \hat{T} shifts the empirical distribution of generated speech toward the target (real) distribution. Since countermeasure systems are trained to reject synthetic distributions and accept real speech, moving the generated distribution closer to the real one can reduce detection performance — i.e., produce a strong, dataset-agnostic adversarial effect.

3.3. Attack Variants

As the set X we used generated audios from ASVspoof2019 dataset (validation part). As the target space Y we investigated two options: hemi-anechoic chamber recordings and diverse recording conditions. As the result, we considered the following attacks.

OT₁: As the target space Y we used bonafide recordings from the ASVspoof2019 dataset built on the VCTK [10].

OT₂: As the target space Y we used the LibriSpeech train-clean-100 dataset [11], because ASVspoof5 used LibriVox data that contains Libri Speech. We select the first 40 speakers (ordered by speaker ID) and, for each, extract 10 random utterances and sort them by duration.

It was noticed in previous research (see, e.g., [4]) that the quality of the voice conversion depends on the length of the target data. Using LibriSpeech dataset was could concatenate several utterances for the same speaker. Evaluation showed that the difference between using VCTK or LibriSpeech is not large (see Table 1), we decided to use OT₂ as the main attack for further analysis.

4. EXPERIMENTAL SETUP

Datasets. We use three public corpora. For constructing the bona fide target pool in our DOT attack (OT₂), we draw from the LibriSpeech Clean, available on Kaggle [12]. For countermeasure (CM) evaluation and cross-dataset transfer, we use ASVspoof2019 accessible on [13], and ASVspoof5 [7]. Unless otherwise stated, we use the official train/dev/eval partitions of each benchmark.

Embeddings. We extract frame-level embeddings using WavLM Large, taking embeddings from the sixth transformer layer accessed through KNN-VC framework [3].

Optimal transport. Discrete OT is solved with entropic regularization via the Sinkhorn algorithm from the POT library [14]. The cosine cost $c(x, y) = 1 - \cos(x, y)$ is used; the regularization parameter is set to $\varepsilon = 0.1$. Top- k barycentric projection produces transported embeddings with $k = 5$.

Vocoder. We reconstruct waveforms from transported embeddings with HiFi-GAN, using the implementation provided with the KNN-VC framework [3].

Countermeasure. For evaluation, we adopt the official AASIST implementation [9] and its pretrained variants.

Evaluation Metric 1: EER We report the equal error rate (EER), i.e., the operating point where the false acceptance rate equals the false rejection rate (see, e.g., [15, Sec. 13]).

Evaluation Metric 2: Distributional similarity. To quantify distributional alignment effects of DOT independently of a specific CM, we compute the *Fréchet Audio Distance* (FAD) [16]. We use `torchvggish` (v0.2) for VGGish embeddings [17], see details in [4].

5. ANALYSIS AND EVALUATION

For evaluation, we used the AASIST model [9], pretrained on the ASVspoof2019 dataset (denoted as AASIST₂₀₁₉), and on ASVspoof5 (denoted as AASIST₅).

Table 1 reports equal error rates (EER) for the generation algorithm A18 from ASVspoof2019 and attack A18 in ASVspoof5, which we denote by A18₅, as well as for the two attacks introduced in the previous section. Algorithms A18 and A18₅ were selected because they exhibit the highest EER within their respective datasets.

Table 1. EER↓ for strongest attacks and proposed attacks.

Attack	AASIST ₂₀₁₉	AASIST ₂₀₁₉ ^{FT}	AASIST ₅	AASIST ₅ ^{FT}
A18	2.614	3.141	77.735	44.951
A18 ₅	0.435	1.443	57.933	2.730
OT ₁	11.111	-	7.268	-
OT ₂	7.925	0.216	11.180	12.586

Column AASIST₂₀₁₉ shows the EER on the validation subset of ASVspoof2019, evaluated with AASIST₂₀₁₉ (i.e., using bonafide data from the ASVspoof2019 validation set).

Column AASIST₅ presents the EER computed with AASIST₅. A notable observation emerges: the strongest attack proposed in ASVspoof5 is detected robustly by the model pretrained on ASVspoof2019. Conversely, most methods from ASVspoof2019 achieve higher EERs than the novel attacks in ASVspoof5 (see also columns (2019) and (5) in Table 2). This asymmetry reflects *adversarial transferability* across models/datasets [18, 19, 20], observed previously in speech systems as well [21, 22].

Column AASIST₂₀₁₉^{FT} shows results after fine-tuning AASIST₂₀₁₉ by including OT₂ examples in the training set of ASVspoof2019.

The final column reports results after fine-tuning AASIST₅ using OT₂ and A18₅ data (see Sec. 5.1 for details).

Table 2 extends this analysis by including attacks A07–A19 (ASVspoof2019) and A17₅–A31₅ (ASVspoof5). Columns (2019) and (5) represent baseline evaluation with AASIST₂₀₁₉ and AASIST₅, while columns (2019)_{OT} and (5)_{OT} show results after applying optimal transport to A07–A19 data.

5.1. Fine-Tuning

Since all generation methods and attacks from ASVspoof5 resulted in very low EER when detected by AASIST₂₀₁₉, we fine-tuned AASIST₂₀₁₉ only with OT₂ data. These examples were obtained by applying optimal transport to generated audio in the ASVspoof2019 training set.

Comparing columns (2019)_{OT} and (2019)_{OT}^{FT} in Table 2 (equivalently, columns AASIST₂₀₁₉ and AASIST₂₀₁₉^{FT} in Table 1), we see that OT₂ attacks are easily detected after fine-tuning. The EER for A18₅ remained largely unchanged.

For AASIST₅, which suffers from a strong A18 attack (and also from A19, though here we focus on adversarial

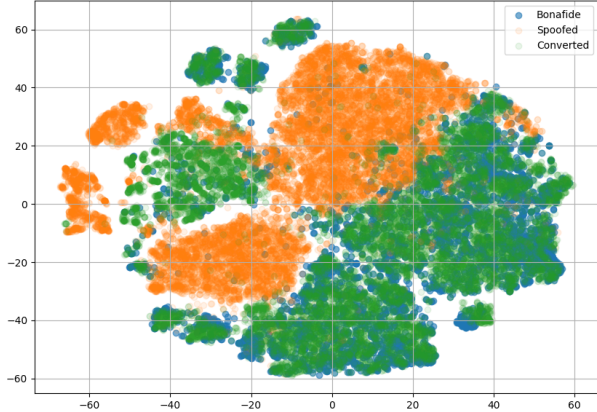


Fig. 2. Bona fide embeddings from LibriSpeech.

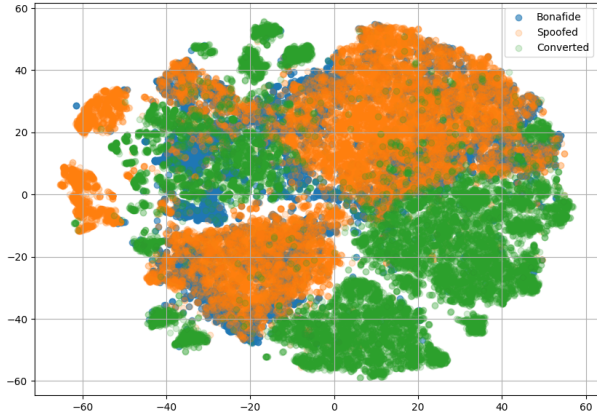


Fig. 3. Bona fide embeddings from ASVspooft2019.

attacks), we fine-tuned using a subset of A18₅ data from the ASVspooft5 evaluation set (12,000 of 27,000 recordings, with the remainder reserved for evaluation) and included OT₂ training data used for fine-tuning AASIST₂₀₁₉.

The comparison between AASIST₅ and AASIST₅^{FT} (Table 1) shows that A18₅ becomes well detected after fine-tuning. However, the OT₂ attack still maintains a high EER.

5.2. The Role of the Vocoder

The relatively low EER for OT₂ in AASIST₅ (Table 1) compared with other attacks (see also Table 2, column (5), rows A17₅–A31₅) may be explained by vocoder overlap. Most of the ASVspooft5 training data are generated with the HiFi-GAN vocoder, which is also used in our attack. This likely explains the elevated EER for methods employing different vocoders, particularly the extremely high EER observed for ASVspooft2019 methods evaluated with AASIST₅ (Table 2, column (5), rows A07–A19).

5.3. The Optimal Transport Property

To further illustrate the effect of optimal transport, we applied t-SNE to VGGish embeddings.

Figure 2 shows embeddings from LibriSpeech bonafide data, ASVspooft2019 generated data (A01–A06), and their

Table 2. EER_↓ before finetuning (2019 and 5); after OT₂ attack (2019_{OT} and 5_{OT}); after attack and finetuning (2019_{OTFT} and 5_{OTFT}).

Attack	2019	2019 _{OT}	2019 _{OTFT}	5	5 _{OT}	5 _{OTFT}
A07	0.52	0.51	0.12	33.28	4.39	10.05
A08	0.42	3.70	0.11	19.90	4.23	9.49
A09	0.00	0.69	0.05	7.79	2.92	7.44
A10	0.86	0.73	0.13	39.42	6.39	14.30
A11	0.18	0.71	0.13	5.65	5.40	13.71
A12	0.78	0.73	0.09	55.41	7.40	13.04
A13	0.15	0.51	0.06	65.51	6.38	15.07
A14	0.15	0.81	0.05	15.34	4.34	8.15
A15	0.55	0.77	0.05	7.30	3.94	8.88
A16	0.65	1.98	0.11	71.97	11.37	17.15
A17	1.26	13.34	0.37	73.26	17.69	12.36
A18	2.61	12.26	0.27	77.73	24.19	14.74
A19	0.65	12.98	0.27	72.57	19.02	14.07
A17 ₅	1.36	-	-	11.43	-	-
A18 ₅	0.43	-	-	51.92	-	-
A19 ₅	0.18	-	-	57.93	-	-
A20 ₅	0.11	-	-	49.78	-	-
A21 ₅	0.72	-	-	13.28	-	-
A22 ₅	1.24	-	-	14.07	-	-
A23 ₅	0.15	-	-	28.81	-	-
A24 ₅	1.39	-	-	10.69	-	-
A25 ₅	0.35	-	-	22.29	-	-
A26 ₅	1.86	-	-	27.41	-	-
A27 ₅	0.18	-	-	24.10	-	-
A28 ₅	0.94	-	-	23.57	-	-
A29 ₅	0.58	-	-	6.83	-	-
A30 ₅	0.25	-	-	39.89	-	-
A31 ₅	0.18	-	-	26.53	-	-

Table 3. FAD_↓ between (Bona fide, Spoof), (Bona fide, OT), and (Spoof, OT).

BF Dataset	BF-Spoof	BF-OT	Spoof-OT
LibriSpeech	4.742	0.508	3.665
ASVspooft2019	1.289	3.402	3.665

OT-transformed versions. The transformed embeddings (Converted) align closely with the LibriSpeech target distribution (Bonafide).

Figure 3 shows embeddings from ASVspooft2019 bonafide data, ASVspooft2019 generated data, and their OT-transformed counterparts. Here, the discrepancy between ASVspooft2019 bonafide data and LibriSpeech becomes evident. This explains why the Fréchet Audio Distance (FAD) between bonafide training data and OT₂ is relatively large (Table 3), and why AASIST₂₀₁₉ readily detects OT₂ after fine-tuning, despite its high pre-finetuning EER.

6. ACKNOWLEDGMENT

The first author thanks You (Neil) Zhang for pointing to the adversarial attacks in ASVspooft5 dataset and bringing to my attention paper [5].

7. REFERENCES

- [1] S. Chen, Ch. Wang, Zh. Chen, et al., “WavLM: Large-scale self-supervised pre-training for full stack speech processing,” *IEEE Journal of Selected Topics in Signal Processing*, vol. 16, no. 6, pp. 1505–1518, 2022.
- [2] M. Baas, B. van Niekerk, and H. Kamper, “Voice conversion with just nearest neighbors,” in *Proc. Interspeech*, Apr. 2023, vol. II, pp. 803–806.
- [3] A. Asadulaev, Korst R., et al., “Optimal transport maps are good voice converters,” in *arXiv preprint arXiv:2411.02402*, 2024.
- [4] Selitskiy A. and Kocharekar M., “Discrete optimal transport and voice conversion,” in *arXiv preprint arXiv:2505.04382*, 2025.
- [5] R. Zhang, J. Wei, et al., “SHDA: sinkhorn domain attention for cross-domain audio anti-spoofing,” *IEEE Transactions on Information Forensics and Security*, vol. 20, pp. 6474–6489, 2024.
- [6] M. Panariello, W. Ge, H. Tak, M. Todisco, and N. Evans, “Malafide: a novel adversarial convolutive noise attack against deepfake and spoofing detection systems,” in *Proc. Interspeech*, Apr. 2023, pp. 2868–2872.
- [7] X. Wang, H. Delgado, et al., “ASVspooF 5: Design, collection and validation of resources for spoofing, deepfake, and adversarial attack detection using crowd-sourced speech,” *Computer Speech & Language*, vol. 95, pp. 1–27, 2026.
- [8] Xin Wang, Junichi Yamagishi, et al., “ASVspooF 2019: A large-scale public database of synthesized, converted and replayed speech,” *Computer Speech & Language*, vol. 64, pp. 101–114, 2020.
- [9] J. Jung, H.-S. Heo, et al., “AASIST: Audio anti-spoofing using integrated spectro-temporal graph attention networks,” in *arXiv preprint arXiv:2110.01200*, 2021.
- [10] J. Yamagishi, C. Veaux, and K. MacDonald, “CSTR VCTK Corpus: english multi-speaker corpus for CSTR voice cloning toolkit (version 0.92),” 2019.
- [11] V. Panayotov, G. Chen, et al., “LibriSpeech: An ASR corpus based on public domain audio books,” in *Proc. ICASSP*, 2015, pp. 5206–5210.
- [12] LibriSpeech Clean, <https://www.kaggle.com/datasets/victorling/librispeech-clean>.
- [13] ASVspooF 2019, <https://www.kaggle.com/datasets/awsaf49/asvspooF-2019-dataset>.
- [14] R. Flamary, N. Courty, et al., “POT: Python optimal transport,” *Journal of Machine Learning Research*, vol. 22, no. 78, pp. 1–8, 2021.
- [15] N. Brümmer and J. du Preez, “Application-independent evaluation of speaker detection,” *Computer Speech & Language*, vol. 20, pp. 230–275, 2006.
- [16] A. Gui, H. Gamper, Braun S., and D. Emmanouilidou, “Adapting Fréchet audio distance for generative music evaluation,” in *Proc. ICASSP*, 2024.
- [17] Sh. Hershey, S. Chaudhuri, et al., “CNN architectures for large-scale audio classification,” in *Proc. ICASSP*, 2017.
- [18] Christian Szegedy, Wojciech Zaremba, Ilya Sutskever, Joan Bruna, Dumitru Erhan, Ian Goodfellow, and Rob Fergus, “Intriguing properties of neural networks,” in *International Conference on Learning Representations (ICLR)*, 2014.
- [19] I. Goodfellow, J. Shlens, and Ch. Szegedy, “Explaining and harnessing adversarial examples,” in *International Conference on Learning Representations (ICLR)*, 2015.
- [20] N. Papernot, P. McDaniel, and I. Goodfellow, “Transferability in machine learning: From phenomena to black-box attacks using adversarial samples,” *arXiv preprint arXiv:1605.07277*, 2016.
- [21] M. Alzantot, B. Balaji, M. Srivastava, et al., “Did you hear that? adversarial examples against automatic speech recognition,” *arXiv preprint arXiv:1801.00554*, 2018.
- [22] X. Liu, X. Wang, M. Sahidullah, et al., “ASVspooF 2021: Towards spoofed and deepfake speech detection in the wild,” *IEEE/ACM Trans. Audio, Speech, Lang. Process.*, vol. 31, pp. 2507–2522, 2023.